NANO LETTERS
Cite This: Nano Lett. XXXX, XXX, XXX−XXX
Letter
pubs.acs.org/NanoLett

Nanodomain Engineering for Programmable Ferroelectric Devices

Alexey Lipatov,[†] Tao Li,[‡,#] Nataliia S. Vorobeva,[†] Alexander Sinitskii,*[,†,§] and Alexei Gruverman*[,‡,§]

[†]Department of Chemistry, University of Nebraska, Lincoln, Nebraska 68588, United States
[‡]Department of Physics and Astronomy, University of Nebraska, Lincoln, Nebraska 68588, United States
[#]Centre for Spintronics and Quantum System, State Key Laboratory for Mechanical Behavior of Materials, School of Materials Science and Engineering, Xi'an Jiaotong University, Xi'an, Shaanxi 710049, People's Republic of China
[§]Nebraska Center for Materials and Nanoscience, University of Nebraska, Lincoln, Nebraska 68588, United States

Supporting Information

ABSTRACT: We introduce a concept of programmable ferroelectric devices composed of two-dimensional (2D) and ferroelectric (FE) materials. It enables precise modulation of the in-plane conductivity of a 2D channel material through nanoengineering FE domains with out-of-plane polarization. The functionality of these new devices has been demonstrated using field-effect transistors (FETs) fabricated with monolayer molybdenum disulfide (MoS_2) channels on the $Pb(Zr,Ti)O_3$ substrates. Using piezoresponse force microscopy (PFM), we show that local switching of FE polarization by a conductive probe can be used to tune the conductivity of the MoS_2 channel. Specifically, patterning of the nanoscale domains with downward polarization creates conductive paths in a resistive MoS_2 channel so that the conductivity of an FET is determined by the number and length of the paths connecting source and drain electrodes. In addition to the device programmability, we demonstrate the device ON/OFF cyclic endurance by successive writing and erasing of conductive paths in a MoS_2 channel. These findings may inspire the development of advanced energy-efficient programmable synaptic devices based on a combination of 2D and FE materials.

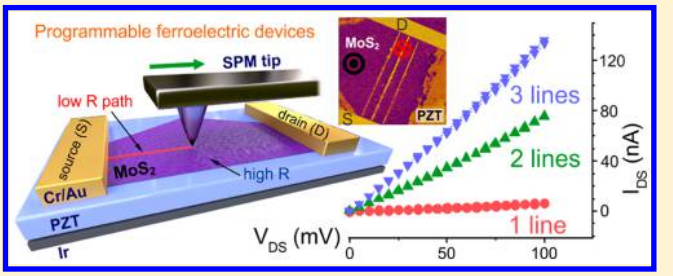

KEYWORDS: *Molybdenum disulfide, lead zirconium titanate, ferroelectric memory, field-effect transistor (FET), domain patterning*

In recent years, there has been a considerable interest in the hybrid electronic structures comprising two-dimensional (2D) and ferroelectric (FE) materials.[1−3] These structures possess appealing characteristics for application in nonvolatile memory and logic devices and may offer low-power, energy-efficient alternatives to CMOS processing. One of such attractive characteristics is memristive functionality, electrically tunable resistivity, which can be used for emulating synaptic functions in neuromorphic computing applications.[4−7] The memristive devices are typically two-terminal structures, in which a layer of a switchable material is sandwiched between two electrodes. In this Letter, we demonstrate a new concept of an electronic device with programmable resistivity based on 2D and FE materials.

The 2D-FE devices can be divided in two general groups based on their architecture and functionality. The first group is ferroelectric field-effect transistors (FeFETs) (Figure 1a), where the in-plane conductivity of a 2D channel material is modulated by the polarization of an FE gate dielectric.[8−11] The second group includes ferroelectric tunnel junctions (FTJs), devices comprising a nanometer-thick FE layer sandwiched between two electrodes (one of which is a 2D material),[12,13] in which the perpendicular-to-plane tunneling conductance can be tuned by switching the ferroelectric polarization (Figure 1b). The original devices of these kinds employed graphene as a channel material (in FeFETs) or a top electrode (in FTJs) and exhibited low ON/OFF ratios due to the semimetallic nature of graphene.[8,14−19] Later on, it was shown that the ON/OFF ratios could be significantly enhanced if graphene was replaced with a semiconducting 2D material with a substantial band gap, such as molybdenum disulfide (MoS_2).[13,20−25] For example, FeFETs employing a MoS_2 device channel on $Pb(Zr,Ti)O_3$ (PZT) exhibit a nonvolatile ON/OFF ratio of over 100, an order of magnitude improvement compared to similar FeFETs based on graphene.[20] In the case of FTJs with the MoS_2 top electrodes, the ON/OFF ratio enhancement compared to their graphene-based counterparts is even more dramatic, by almost 2 orders of magnitude. In addition, it was reported that the coupling between ferroelectric polarization and conductivity of MoS_2 resulted in an asymmetric and spatially confined switching behavior in MoS_2−$BaTiO_3$ FTJs, which allowed fine-tuning of the resistive states achieved via generation of stable sequential domain patterns in $BaTiO_3$

Received: February 15, 2019
Revised: March 25, 2019
Published: April 3, 2019

DOI: 10.1021/acs.nanolett.9b00673
Nano Lett. XXXX, XXX, XXX−XXX

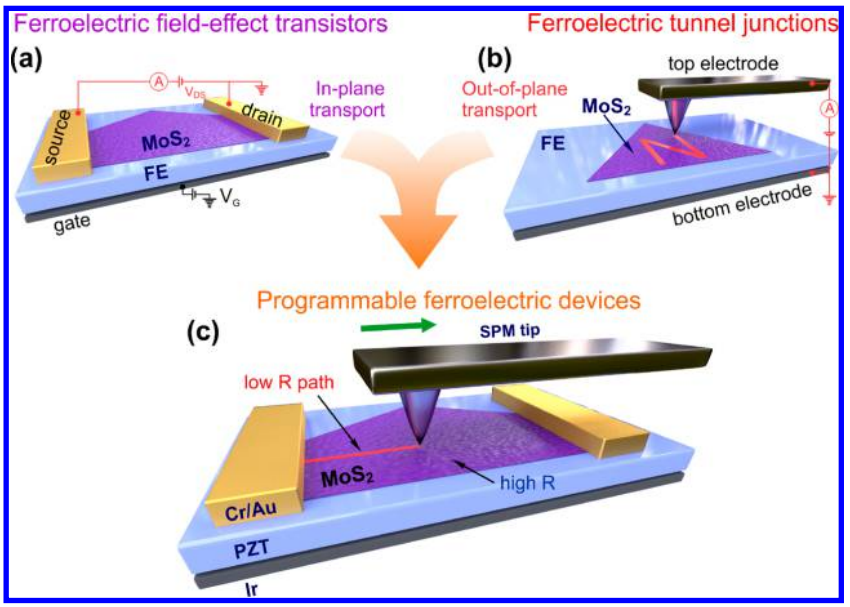

Figure 1. General concept of a programmable MoS_2-ferroelectric device realized through nanodomain engineering. (a) Scheme of an FeFET with a MoS_2 channel and an FE film as a gate dielectric. Modulated by gate voltage, the in-plane channel conductivity is measured using drain and source electrodes. (b) Scheme of an FTJ device comprising an FE substrate and a MoS_2 flake, where ferroelectric polarization is locally switched by an electrical bias applied through the PFM tip. (c) Scheme of a programmable FeFET where the in-plane conductivity is tuned by writing a conductive path (red line) in the MoS_2 channel through local polarization switching in the FE substrate.

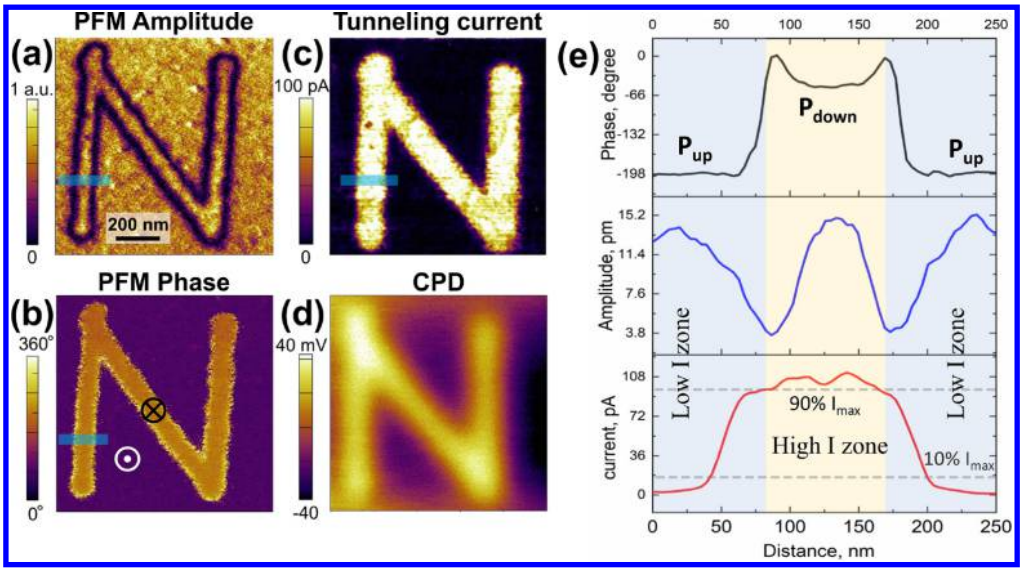

Figure 2. Control of the electronic properties of the MoS_2–BTO FTJ by nanoscale domain patterning. (a, b) PFM amplitude (a) and phase (b) images of the N-shaped domain pattern created by scanning the tip at the +4 V dc bias with a 500 nm/s speed. (c, d) Corresponding tunneling current (c) and contact potential difference (CPD) (d) maps. (e) From top to bottom: line profiles of the PFM phase, PFM amplitude, and tunneling current taken along the blue line in panels b, a, and c, respectively.

(BTO) (Figure 1b), adding memristive functionality to the FTJ devices.[13] Here, we extend the concept of nanoscale domain engineering for resistance control to the hybrid 2D-FE FET devices (Figure 1c). Using the scanning probe microscopy (SPM) approach, we demonstrate a precise reversible modulation of the in-plane electronic transport in the MoS_2–PZT FETs by creating conductive domain paths of a specific geometry.

While Figure 1c demonstrates a general concept of a programmable MoS_2–FE device, below we provide a detailed description of nanodomain engineering by an electrical bias applied to the MoS_2 layer via a conductive SPM tip as a way to control the device conducting state. This approach makes use of the asymmetric nature of polarization reversal in the MoS_2–FE structures and the dependence of the MoS_2 electronic properties on the FE polarization direction. Specifically, it has been shown[11,13] that the downward (toward the bottom electrode) FE polarization drives a MoS_2 flake into an electrically conductive state, which allows complete switching of polarization from the downward (P_{down}) to the upward (P_{up}) state in the whole volume of an FE material underneath MoS_2 upon application of a single negative pulse from an SPM tip (Figure 1b).[13] In turn, the upward FE polarization makes MoS_2 more insulating so that application of a positive pulse

DOI: 10.1021/acs.nanolett.9b00673
Nano Lett. XXXX, XXX, XXX–XXX

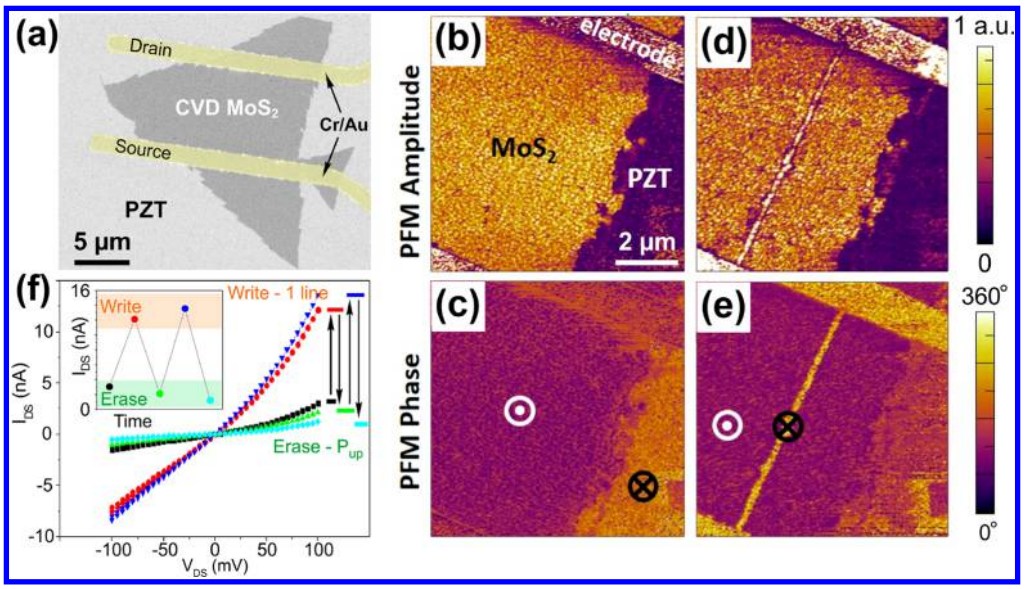

Figure 3. Nanoscale domain engineering in MoS_2−PZT FeFET. (a) "Scanning electron microscopy image of the device comprising a CVD-grown triangular crystal of monolayer MoS_2 bridging two Cr/Au electrodes on a PZT substrate. (b, c) PFM amplitude (b) and PFM phase (c) images of the MoS_2−PZT device. The PZT polarization under the MoS_2 flake is oriented upward, while the bare PZT film around the flake is polarized downward. (d, e) PFM amplitude (d) and PFM phase (e) images of the MoS_2−PZT device with a conductive path in the MoS_2 channel connecting the drain and source electrodes created by local domain switching in the PZT film. (f) I_{DS}−V_{DS} curves acquired during a cyclic endurance test of resistive switching performed by writing and erasing a single conductive path in the MoS_2 channel. Inset: I_{DS} values extracted from the main panel f at V_{DS} = 100 mV.

results only in local switching of the polarization to the downward state right under the tip. This behavior is illustrated in Figure 2, where the N-shaped downward-oriented domain was created in the MoS_2/BTO FTJ by scanning with the tip under a positive bias of 4 V. Comparison of the domain pattern visualized using piezoresponse force microscopy (PFM) (Figure 2a,b) and a corresponding conducting atomic force microscopy (CAFM) map (Figure 2c) shows that BTO polarization strongly affects the out-of-plane conductivity of the MoS_2−BTO heterostructure: a much higher current (by almost 2 orders of magnitude) is detected in the region with the downward polarization P_{down}. Kelvin probe force microscopy (KPFM) measurements reveal the corresponding variations in the contact potential difference (CPD) of MoS_2 caused by the charge accumulation/depletion in MoS_2 by the opposite polarization charges of the underneath BTO film (Figure 2d). Cross-sectional analysis of the PFM, CAFM, and KPFM maps (Figure 2e) shows a clear correlation between the polarization, local conductivity, and surface potential in the MoS_2−BTO heterostructure.

The same nanodomain engineering approach can be applied to modulate the in-plane conductivity of the MoS_2−PZT FETs (Figure 1a) with a single-crystalline monolayer MoS_2 channel bridging source (S) and drain (D) electrodes (Figure 3a). Polycrystalline 100 nm-thick (001)-oriented tetragonal $PbZr_{0.4}Ti_{0.6}O_3$ ferroelectric films used in this study were grown by metal−organic chemical vapor deposition (CVD) on the Ir/TiO_2/SiO_2/Si substrate. The CVD-grown monolayer MoS_2 flakes,[26] characterized by Raman spectroscopy,[27] were placed onto the PZT surface using the wet transfer technique.[12] The Cr/Au source and drain electrodes contacting MoS_2 flakes were fabricated by the standard electron beam lithography and electron beam evaporation. Details of the experimental methods and device fabrication are given in the Supporting Information.

Figure 3b,c shows PFM images of the MoS_2−PZT device. The PZT film underneath the MoS_2 flake initially polarized downward was switched to the upward direction by the application of a −5 V pulse to the flake. The upward PZT polarization yields the OFF (low conductance) state of the FET with the drain−source current (I_{DS}) at the level of 3.0 nA at V_{DS} = 100 mV (Figure 3f). Scanning a region between the planar source/drain electrodes with the tip under a +5 V dc bias at 500 nm/s results in a 200 nm-wide linear domain with the downward polarization (Figure 3d,e). The associated change in local conductivity of MoS_2 results in the appearance of a conducting channel between the source and drain electrodes, leading to an increase of I_{DS} up to 12.3 nA at V_{DS} = 100 mV (see the red I_{DS}−V_{DS} dependence in Figure 3f), thereby driving the device to the ON state. The written domain width strongly depends on the writing bias but shows a relatively weak dependence on the tip scanning speed during writing (see Figures S1 and S2). This conductive path can be severed by applying a short negative pulse and then restored again by scanning with a positively biased SPM tip (see Figure S1). Erasure occurs when a negative pulse of −5 V is applied to the MoS_2 flake, switching the polarization of the entire PZT volume under the flake to the upward state.

Endurance of conductance modulation via the domain engineering has been tested by performing several cycles of writing and complete erasing of a domain line (Figure 3f). The high-resistance state exhibits I_{DS} in the range of 1−3 nA at V_{DS}= 100 mV, while for the low-resistance state with a single domain line the I_{DS} is in the range of 12−14 nA at V_{DS} = 100 mV (see the inset in Figure 3f). The I_{DS}−V_{DS} curves for the OFF and ON states are reproducible from cycle to cycle. This experiment proves the reliability and programmability of the nanodomain engineering method as a resistance-modulation procedure for the hybrid 2D-FE devices.

DOI: 10.1021/acs.nanolett.9b00673
Nano Lett. XXXX, XXX, XXX−XXX

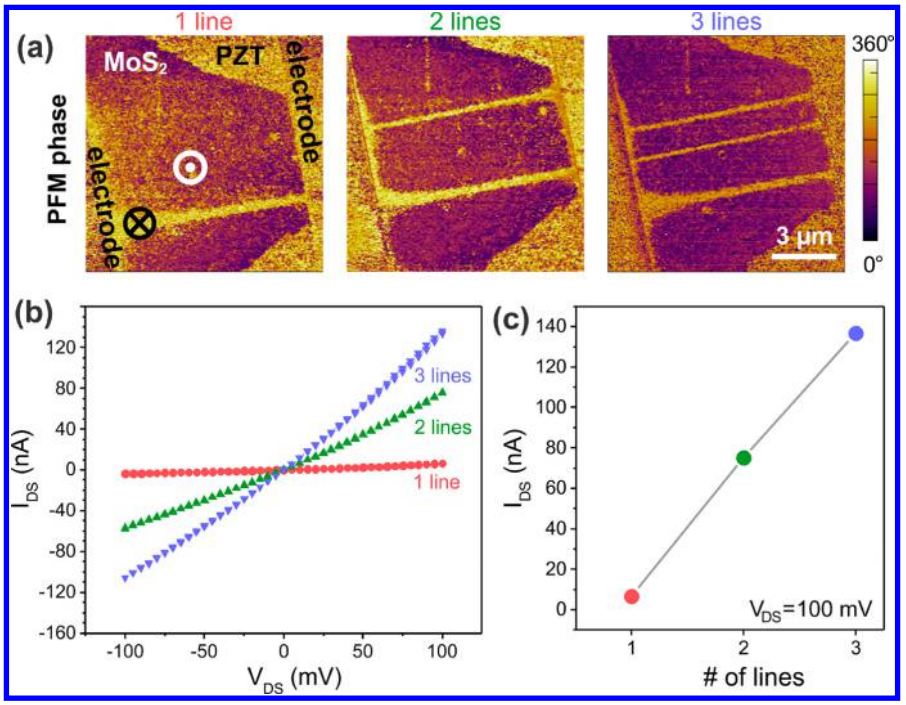

Figure 4. Tunability of the in-plane resistance states in MoS_2−PZT FeFET. (a) PFM phase images of a MoS_2−PZT FeFET with one, two, and three conductive paths gated by the domains with the downward polarization, while the rest of the MoS_2 channel remains in the high-resistance state due to the upward polarization of PZT. (b) I_{DS}−V_{DS} curves for different numbers of conductive paths. (c) Dependence of the I_{DS} values measured at V_{DS} = 100 mV on the number of conductive paths.

PFM allows patterning arbitrarily shaped conducting paths, as illustrated by Figure S3, where a number of downward polarized domain lines were created in the channel of the MoS_2−PZT FET. Thus, nanoscale domain engineering allows for fine-tunability of resistance in the MoS_2−PZT FETs. Figure 4a shows PFM images recorded after creating several downward polarized domain lines by the SPM tip scanning under the positive bias of 5 V. The in-plane conductivity measurements, which were performed after writing each P_{down} domain line, reveal the I_{DS} currents of 6.5, 75, and 136 nA at V_{DS} = 100 mV for one, two, and three domain lines, respectively (Figure 4b). The device conductivity increases linearly with the number of lines as shown in Figure 4c, yielding the maximum ON/OFF ratio of about 130. The estimated ON/OFF ratio for the fully switched PZT underneath the MoS_2 flake is of the order of 1500.

In summary, we demonstrated the concept of a new programmable semiconductor device with a 2D channel and ferroelectric gating that enables precise modulation of the in-plane conductivity through the nanoengineering of ferroelectric domains with out-of-plane polarization. Functionality of these devices was demonstrated using MoS_2-based FETs fabricated on the PZT substrates. Anisotropic switching behavior of the MoS_2−PZT heterostructures enables the PFM patterning of arbitrarily shaped nanoscale downward domains, allowing local control of the MoS_2 conductivity. It is shown that generation of a conductive path in the MoS_2 layer connecting the source and drain electrodes by polarization switching in the predetermined regions of the underlying PZT film drives the MoS_2−PZT FET device from an OFF resistive state to an ON resistive state. The cyclic endurance and reproducibility of the resistance switching have been demonstrated by successive writing and erasing of the conductive paths in the MoS_2 channel. The ON state conductivity can be further modulated by creating a different number of conducting paths of variable geometry (i.e., shape and width) using a proper combination of the electrical bias and scanning trajectories, which opens a possibility for the development of novel synapse devices with multiple resistive states. Furthermore, the experimentally demonstrated programmability of the MoS_2−PZT FETs may inspire the development of innovative designs for energy-efficient synaptic devices.

■ ASSOCIATED CONTENT

Supporting Information

The Supporting Information is available free of charge on the ACS Publications website at DOI: 10.1021/acs.nanolett.9b00673.

Materials and methods, images and analysis of CVD-grown MoS_2, and additional PFM images for different domain patterning parameters (PDF)

■ AUTHOR INFORMATION

Corresponding Authors

*E-mail: sinitskii@unl.edu.
*E-mail: alexei_gruverman@unl.edu.

ORCID

Alexey Lipatov: 0000-0001-5043-1616
Alexander Sinitskii: 0000-0002-8688-3451
Alexei Gruverman: 0000-0003-0492-2750

Author Contributions

A.L. and T.L. contributed equally. All authors have given approval to the final version of the manuscript.

Notes

The authors declare no competing financial interest.

DOI: 10.1021/acs.nanolett.9b00673
Nano Lett. XXXX, XXX, XXX−XXX

■ ACKNOWLEDGMENTS

This work was supported by the National Science Foundation (NSF) through the Nebraska Materials Research Science and Engineering Center (MRSEC) (grant no. DMR-1420645). This research was performed in part in the Nebraska Nanoscale Facility: National Nanotechnology Coordinated Infrastructure, which was supported by the NSF (ECCS-1542182) and the Nebraska Research Initiative.

■ REFERENCES

(1) Hong, H. Emerging ferroelectric transistors with nanoscale channel materials: the possibilities, the limitations. *J. Phys.: Condens. Matter* **2016**, *28*, 103003.
(2) Zhou, C.; Chai, Y. Ferroelectric-Gated Two-Dimensional-Material-Based Electron Devices. *Adv. Electron. Mater.* **2017**, *3*, 1600400.
(3) Jie, W.; Hao, J. Graphene-Based Hybrid Structures Combined with Functional Materials of Ferroelectrics and Semiconductors. *Nanoscale* **2014**, *6*, 6346−6362.
(4) Strukov, D. B.; Snider, G. S.; Stewart, D. R.; Williams, R. S. The missing memristor found. *Nature* **2008**, *453*, 80−83.
(5) Jo, S. H.; Chang, T.; Ebong, I.; Bhadviya, B. B.; Mazumder, P.; Lu, W. Nanoscale Memristor Device as Synapse in Neuromorphic Systems. *Nano Lett.* **2010**, *10*, 1297−1301.
(6) Kuzum, D.; Yu, S.; Wong, P. H. S. Synaptic electronics: materials, devices and applications. *Nanotechnology* **2013**, *24*, 382001.
(7) Zidan, M. A.; Strachan, J. P.; Lu, W. D. The future of electronics based on memristive systems. *Nature Electronics* **2018**, *1*, 22−29.
(8) Zheng, Y.; Ni, G.-X.; Toh, C.-T.; Zeng, M.-G.; Chen, S.-T.; Yao, K.; Özyilmaz, B. Gate-Controlled Nonvolatile Graphene-Ferroelectric Memory. *Appl. Phys. Lett.* **2009**, *94*, 163505.
(9) Hong, X.; Hoffman, J.; Posadas, A.; Zou, K.; Ahn, C. H.; Zhu, J. Unusual Resistance Hysteresis in n-Layer Graphene Field Effect Transistors Fabricated on Ferroelectric $Pb(Zr_{0.2}Ti_{0.8})O_3$. *Appl. Phys. Lett.* **2010**, *97*, 033114.
(10) Baeumer, C.; Rogers, S. P.; Xu, R. J.; Martin, L. W.; Shim, M. Tunable Carrier Type and Density in Graphene/$PbZr_{0.2}Ti_{0.8}O_3$ Hybrid Structures through Ferroelectric Switching. *Nano Lett.* **2013**, *13*, 1693−1698.
(11) Lipatov, A.; Fursina, A.; Vo, T. H.; Sharma, P.; Gruverman, A.; Sinitskii, A. Polarization-Dependent Electronic Transport in Graphene/$Pb(Zr,Ti)O_3$ Ferroelectric Field-Effect Transistors. *Adv. Electron. Mater.* **2017**, *3*, 1700020.
(12) Lu, H.; Lipatov, A.; Ryu, S.; Kim, D. J.; Lee, H.; Zhuravlev, M. Y.; Eom, C. B.; Tsymbal, E. Y.; Sinitskii, A.; Gruverman, A. Ferroelectric Tunnel Junctions with Graphene Electrodes. *Nat. Commun.* **2014**, *5*, 5518.
(13) Li, T.; Sharma, P.; Lipatov, A.; Lee, H.; Lee, J.-W.; Zhuravlev, M. Y.; Paudel, T. R.; Genenko, Y. A.; Eom, C.-B.; Tsymbal, E. Y.; Sinitskii, A.; Gruverman, A. Polarization-Mediated Modulation of Electronic and Transport Properties of Hybrid MoS_2−$BaTiO_3$−$SrRuO_3$ Tunnel Junctions. *Nano Lett.* **2017**, *17*, 922−927.
(14) Hong, X.; Posadas, A.; Zou, K.; Ahn, C. H.; Zhu, J. High-Mobility Few-Layer Graphene Field Effect Transistors Fabricated on Epitaxial Ferroelectric Gate Oxides. *Phys. Rev. Lett.* **2009**, *102*, 136808.
(15) Hong, X.; Hoffman, J.; Posadas, A.; Zou, K.; Ahn, C. H.; Zhu, J. Unusual resistance hysteresis in n-layer graphene field effect transistors fabricated on ferroelectric $Pb(Zr_{0.2}Ti_{0.8})O_3$. *Appl. Phys. Lett.* **2010**, *97*, 033114.
(16) Zheng, Y.; Ni, G.-X.; Toh, C.-T.; Tan, C.-Y.; Yao, K.; Özyilmaz, B. Graphene Field-Effect Transistors with Ferroelectric Gating. *Phys. Rev. Lett.* **2010**, *105*, 166602.
(17) Song, E. B.; Lian, B.; Kim, S. M.; Lee, S.; Chung, T. K.; Wang, M. S.; Zeng, C. F.; Xu, G. Y.; Wong, K.; Zhou, Y.; Rasool, H. I.; Seo, D. H.; Chung, H. J.; Heo, J.; Seo, S.; Wang, K. L. Robust bi-stable memory operation in single-layer graphene ferroelectric memory. *Appl. Phys. Lett.* **2011**, *99*, 042109.
(18) Lee, W.; Kahya, O.; Toh, C. T.; Özyilmaz, B.; Ahn, J.-H. Flexible graphene−PZT ferroelectric nonvolatile memory. *Nanotechnology* **2013**, *24*, 475202.
(19) Rajapitamahuni, A.; Hoffman, J.; Ahn, C. H.; Hong, X. Examining Graphene Field Effect Sensors for Ferroelectric Thin Film Studies. *Nano Lett.* **2013**, *13*, 4374−4379.
(20) Lipatov, A.; Sharma, P.; Gruverman, A.; Sinitskii, A. Optoelectrical Molybdenum Disulfide (MoS_2)—Ferroelectric Memories. *ACS Nano* **2015**, *9*, 8089−8098.
(21) Zhang, X. W.; Xie, D.; Xu, J. L.; Sun, Y. L.; Li, X.; Zhang, C.; Dai, R. X.; Zhao, Y. F.; Li, X. M.; Li, X.; Zhu, H. W. MoS_2 Field-Effect Transistors with Lead Zirconate-Titanate Ferroelectric Gating. *IEEE Electron Device Lett.* **2015**, *36*, 784−786.
(22) Ko, C.; Lee, Y.; Chen, Y.; Suh, J.; Fu, D.; Suslu, A.; Lee, S.; Clarkson, J. D.; Choe, H. S.; Tongay, S.; Ramesh, R.; Wu, J. Ferroelectrically Gated Atomically Thin Transition-Metal Dichalcogenides as Nonvolatile Memory. *Adv. Mater.* **2016**, *28*, 2923−2930.
(23) Sun, Y.; Dan, X.; Xiaowen, Z.; Jianlong, X.; Xinming, L.; Xian, L.; Ruixuan, D.; Xiao, L.; Peilian, L.; Xingsen, G.; Hongwei, Z. Temperature-dependent transport and hysteretic behaviors induced by interfacial states in MoS_2 field-effect transistors with lead-zirconate-titanate ferroelectric gating. *Nanotechnology* **2017**, *28*, 045204.
(24) Lu, Z.; Serrao, C.; Khan, A. I.; You, L.; Wong, J. C.; Ye, Y.; Zhu, H.; Zhang, X.; Salahuddin, S. Nonvolatile MoS_2 field effect transistors directly gated by single crystalline epitaxial ferroelectric. *Appl. Phys. Lett.* **2017**, *111*, 023104.
(25) Lu, Z.; Serrao, C.; Khan, A. I.; Clarkson, J. D.; Wong, J. C.; Ramesh, R.; Salahuddin, S. Electrically induced, non-volatile, metal insulator transition in a ferroelectric-controlled MoS_2 transistor. *Appl. Phys. Lett.* **2018**, *112*, 043107.
(26) Zobel, A.; Boson, A.; Wilson, P. M.; Muratov, D. S.; Kuznetsov, D. V.; Sinitskii, A. Chemical vapour deposition and characterization of uniform bilayer and trilayer MoS_2 crystals. *J. Mater. Chem. C* **2016**, *4*, 11081−11087.
(27) Li, H.; Zhang, Q.; Yap, C. C. R.; Tay, B. K.; Edwin, T. H. T.; Olivier, A.; Baillargeat, D. From Bulk to Monolayer MoS_2: Evolution of Raman Scattering. *Adv. Funct. Mater.* **2012**, *22*, 1385−1390.

DOI: 10.1021/acs.nanolett.9b00673
Nano Lett. XXXX, XXX, XXX−XXX